Structure and Function of the Phenazine Biosynthesis Protein PhzF from *Pseudomonas fluorescens* 2-79‡

James F. Parsons,|| Fenhong Song,|| Lisa Parsons,|| Kelly Calabrese,|| Edward Eisenstein,*,||,⊥ and Jane E. Ladner*,||

Center for Advanced Research in Biotechnology, University of Maryland Biotechnology Institute, National Institute of Standards and Technology, 9600 Gudelsky Drive, Rockville, Maryland 20850, and Departments of Chemistry and Biochemistry, University of Maryland Baltimore County, Baltimore, Maryland 21228

Received May 10, 2004; Revised Manuscript Received July 15, 2004

ABSTRACT: Phenazines, including pyocyanin and iodonin, are biologically active compounds that are believed to confer producing organisms with a competitive growth advantage, and also are thought to be virulence factors in certain diseases including cystic fibrosis. The basic, tricyclic phenazine ring system is synthesized in a series of poorly characterized steps by enzymes encoded in a seven-gene cistron in *Pseudomonas* and other organisms. Despite the biological importance of these compounds, and our understanding of their mode of action, the biochemistry and mechanisms of phenazine biosynthesis are not well resolved. Here we report the 1.8 Å crystal structure of PhzF, a key enzyme in phenazine biosynthesis, solved by molecular replacement. PhzF is structurally similar to the lysine biosynthetic enzyme diaminopimelate epimerase, sharing an unusual fold consisting of two nearly identical domains with the active site located in an occluded cleft between the domains. Unlike diaminopimelate epimerase, PhzF is a dimer in solution. The two apparently independent active sites open toward opposite sides of the dimer and are occupied by sulfate ions in the structure. In vitro experiments using a mixture of purified PhzF, -A, -B, and -G confirm that phenazine-1-carboxylic acid (PCA) is readily produced from *trans*-2,3-dihydro-3-hydroxyanthranilic acid (DHHA) without aid of other cellular factors. PhzA, -B, and -G have no activity toward DHHA. However, in the presence of PhzF, individually or in combinations, they accelerate the formation of PCA from DHHA and therefore appear to function after the action of PhzF. Surprisingly, PhzF is itself capable of producing PCA, albeit slowly, from DHHA. These observations suggest that PhzF catalyzes the initial step in the conversion of DHHA to PCA, probably via a rearrangement reaction yielding the more reactive 3-oxo analogue of DHHA, and that subsequent steps can occur spontaneously. A hypothetical model for how DHHA binds to the PhzF active site suggests that Glu45 and Asp208 could act as general acid−base catalysts in a rearrangement reaction. Given that four reactions lie between DHHA and PCA, ketone formation, ring formation, decarboxylation, and oxidation, we hypothesize that the similar PhzA and -B proteins catalyze ring formation and thus may be more than noncatalytic accessory proteins. PhzG is almost certainly an oxidase and is predicted to catalyze the final oxidation/aromatization reaction.

Several species of *Pseudomonas*, including the human pathogen *P. aeruginosa*, produce secondary metabolites known as phenazines (Scheme 1). The phenazine family consists of over 100 compounds, all of which have the characteristic tricyclic ring system shown in Scheme 1. Phenazines are redox active compounds that engage in reactions yielding superoxide ions, peroxide ions, and hydroxyl radicals (*1*, *2*). These toxic species control the growth of other microorganisms in the local environment to provide *Pseudomonas* with a competitive growth advantage, and they may enhance the ability of these pathogens to colonize human and other tissues.

Scheme 1: Pathway for Conversion of Chorismic Acid to Phenazine-1-Carboxylate

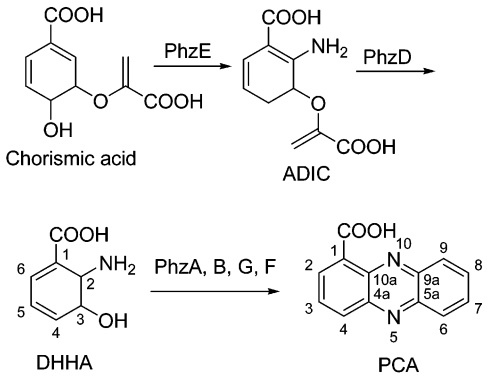

The important metabolic intermediate chorismic acid (*3*) is a phenazine precursor. Two seven-gene *phzABCDEFG* operons have been identified in both *P. fluorescens* 2-79 and *P. aeruginosa* that encode the proteins necessary for the conversion of chorismic acid to phenazine-1-carboxylate

‡ Coordinates for PhzF have been deposited in the RCSB Protein Data Bank as entry 1T6K.

* To whom correspondence should be addressed. Mailing address: Center for Advanced Research in Biotechnology, 9600 Gudelsky Drive, Rockville, MD 20850. Phone (E.E.): 301-738-6244. Fax: 301-738-6255. E-mail addresses: jane.ladner@nist.gov; edd@carb.nist.gov.

|| Center for Advanced Research in Biotechnology.

⊥ University of Maryland Baltimore County.

10.1021/bi049059z CCC: $27.50
Published on Web 09/09/2004

(PCA)[1] (*1*, *4*). The functions of PhzC, -D, and -E either have been established experimentally or can be inferred on the basis of similarity to proteins of known function. PhzC appears to be a deoxy-arabinoheptulosonate-7-phosphate (DAHP) synthase that acts to ensure that adequate chorismate is available for phenazine synthesis by circumventing an otherwise tightly regulated step in chorismate biosynthesis (*5*). BLAST (*6*) analysis of the PhzE sequence indicates that it is similar to bacterial anthranilate synthases, which catalyze the related conversion of chorismate to anthranilate. However, unlike anthranilate synthase, which sequesters an aminodeoxyisochorismate (ADIC) intermediate (*7*), ADIC is the final product of the PhzE-catalyzed transformation of chorismate (Scheme 1). Biochemical evidence has shown that PhzD catalyzes the conversion of ADIC to *trans*-2,3-dihydro-3-hydroxyanthranilic acid (DHHA) (*8*). DHHA is then converted to PCA in several poorly characterized steps involving the condensation of two DHHA molecules to form the phenazine ring system. McDonald and co-workers have proposed that PhzG catalyzes the oxidation of DHHA to the corresponding 3-oxo species, which then dimerizes in a reaction catalyzed by PhzF (Scheme 1) (*9*). No direct evidence supporting this mechanism has been presented, but several lines of evidence do support parts of the proposal. PhzG is a pyridoxine-5′-phosphate oxidase (PdxH) homolog. The rmsd between the PhzG structure (PDB code 1T9M, manuscript in preparation) and PdxH (PDB code 1DNL) is 1.4 Å for all Cα atoms, and the substrate for PdxH, pyridoxine phosphate, is reasonably similar to DHHA. Also, oxidation of DHHA to the 3-oxo species prior to dimerization is a chemically reasonable mechanism for the reaction. However, our inability to detect any activity with PhzG toward DHHA led us to look for other possible roles for PhzG and, consequently, other proposals that could account for the formation of PCA from DHHA.

To further characterize the details of the phenazine biosynthesis, in particular the formation of the initial tricyclic species, we report the enzymological properties and the crystal structure of PhzF from *Pseudomonas fluorescens* 2-79 at 1.8 Å resolution. The fold of PhzF is similar to that of diaminopimelate (DAP) epimerase (*10*) and two proteins of unknown function. Unlike DAP epimerase, PhzF is a dimer in solution. NMR, mass spectrometry, and UV spectroscopy show that, surprisingly, phenazine-1-carboxylate is produced from DHHA in the presence of PhzF alone. The conversion is slow, however, and PhzA,-B, and -G accelerate the process significantly. Dimerization of DHHA most likely proceeds via a ketone, and we predict that PhzF generates a reactive 3-ketone product from DHHA, probably by allylic rearrangement, a process that is analogous to the reaction catalyzed by DAP epimerase. Substrate dimerization is further predicted to occur spontaneously at a slow rate in the absence of a catalyst and more rapidly in a process facilitated by PhzA and PhzB with PhzG catalyzing a final oxidation/aromatization step.

MATERIALS AND METHODS[2]

Cloning. P. fluorescens was obtained from the United States Department of Agriculture, Agricultural Research Service culture collection (Peoria, IL). The DNA encoding *P. fluorescens* PhzF was amplified from *P. fluorescens* genomic DNA using synthetic primers compatible with the published *phzF* sequence (*4*). *Nde*I and *Hin*dIII restriction enzyme sites were included in each case and the digested fragments were ligated into the similarly digested expression vector pET28a (Novagen). Each of the other *phz* operon genes were cloned in an identical manner.

trans-2,3-Dihydro-3-hydroxyanthranilic Acid (DHHA). DHHA was prepared by treating 2-amino-2-deoxyisochorismate (*8*) with PhzD enzyme in 50 mM ammonium acetate (pH 7). Enzyme was removed by filtration, and the DHHA was purified on an AG1-X8 column (Bio-Rad; hydroxide form) equilibrated at pH 10. DHHA was eluted with 1 M ammonium acetate, lyophilized multiple times from either H_2O or D_2O, and stored at −80 °C. Characterization by ^1H NMR and UV spectroscopy was consistent with previous observations (*9*).

Analysis of Enzymatic Activities. Enzymatic activity was typically measured in 50 mM potassium phosphate (pH 7.4) at room temperature. Analytical scale reactions typically contained 0.5−1 μM enzyme and 100 μM DHHA. Preparative scale reactions were run overnight and typically contained 20−50 mM DHHA and 5−10 μM enzyme.

Isolation of Reaction Products. Reaction products were isolated by repeated extraction of aqueous reactions with methylene chloride. Samples were dried under a nitrogen stream, and the residue was redissolved in either methanol for HPLC, MS, and UV experiments or $CDCl_3$ for NMR experiments.

Instrumental Methods. All mass spectra were acquired on a Mariner electrospray ionization instrument (Applied Biosystems) operating in positive ion mode. Direct injections were made at 1−3 μL/min in 90−100% methanol, 1% acetic acid.

NMR spectra were acquired at 25 °C using either a Bruker Avance 600 or a Bruker DMX-500 instrument, both equipped with triple resonance probes. All spectra were acquired in $CDCl_3$. Proton chemical shifts were referenced either to TMS or $CHCl_3$. Carbon chemical shifts for nuclei at natural abundance were determined indirectly due to the small amounts of material available. Proton and carbon shifts were correlated by analyzing data from a ^{13}C HSQC experiment. ^1H-^{13}C HMBC (*11*) spectroscopy was used to unambiguously assign proton resonances, particularly for H2 and H4 of PCA.

HPLC was used to separate and identify reaction products based on retention time. A 4.6 mm × 150 mm μbondapak C18 reversed phase column (Waters) was used in conjunction with a Gilson binary gradient HPLC system. The separation method was similar to that described previously (*1*) except the aqueous phase was 20 mM ammonium acetate (pH 4.5).

[1] Abbreviations: PCA, phenazine-1-carboxylate; ADIC, 2-amino-2-deoxyisochorismate; DHHA, *trans*-2,3-dihydro-3-hydroxyanthranilic acid; DAP, diaminopimelate; MS, mass spectrometry; HSQC, heteronuclear single quantum coherence; HMBC, heteronuclear multiple bond correlation; TMS, tetramethylsilane; ppm, parts per million; DTT, dithiothreitol; EDTA, ethylenediaminetetraacetic acid; PEG, poly(ethylene glycol).

[2] Certain commercial materials, instruments, and equipment are identified in this manuscript in order to specify the experimental procedure as completely as possible. In no case does such identification imply a recommendation or endorsement by the National Institute of Standards and Technology nor does it imply that the materials, instruments, or equipment identified is necessarily the best available for the purpose.

The flow rate was 0.8 mL/min, and analytical injections were typically 20 μL or less.

Protein Expression and Purification. *P. fluorescens* PhzF was expressed in *Escherichia coli* strain BL21(DE3). Cells harboring the pET28a-*phzF* plasmid were grown in shaker flasks at 35 °C in autoinduction medium containing 100 μg/mL kanamycin. Cells were harvested after 16 h and lysed by sonication in 50 mM KH_2PO_4, 200 mM NaCl, 10 mM imidazole, and 10% glycerol (pH 8.0). PhzF was purified by Ni−NTA affinity chromatography as directed by the resin manufacturer (Novagen). Fractions containing pure PhzF were pooled and dialyzed 50 mM Hepes, 1 mM EDTA, 1 mM DTT, 10% glycerol (pH 7.6), concentrated to ∼17 mg/mL, and stored at −80 °C. Yield was about 50 mg pure enzyme per liter of culture. PhzA, PhzB, and PhzG were expressed and purified in a similar manner except glycerol was not used. Additionally, for each protein except PhzF, the histidine affinity tag was removed by thrombin digestion, and the cleaved tag and thrombin were removed from the reaction by passage over a *p*-aminobenzamidine column and a second passage through a reequilibrated Nickel column.

Molecular Weight from Laser Light Scattering. The solution molecular mass of PhzF was determined by a combination of laser light scattering and interferometric refractometry using a DAWN EOS and Optilab DSP system (Wyatt). Samples were subjected to gel filtration chromatography (Shodex KW-803; 300 mm × 8 mm) prior to in-line analysis. Molecular weights were calculated using ASTRA software.

Crystallization. Crystals of PhzF were grown at room temperature by the hanging drop vapor diffusion method. The well solution was 0.20 M ammonium sulfate, 0.10 M sodium citrate, pH 5.2, and 18% (w/v) PEG 4000. The drops were made by adding equal volumes of protein solution and well solution. The protein concentration was typically ∼20 mg/mL before mixing.

Data Collection. Diffraction data were collected using a Rigaku Micro Max 007 rotating anode generator and a Rigaku RAXIS IV^{2+} detector (Rigaku/MSC, The Woodlands, TX). The crystals were cooled to 105 K with an Oxford Cryosystems cryocooler and were cryoprotected by the addition of 50% PEG 4000 to the reservoir solution in a ratio of 1:1. Diffraction data were processed with CrystalClear/d*Trek (*12*). Statistics for the data collection and refinement are shown in Table 1.

Structure Determination. A reasonable value, 2.35 $Å^3$/Da, was obtained for Matthews constant assuming one polypeptide chain in the asymmetric unit. A BLAST (*6*) search of the PDB (*13*) indicated that PhzF has significant sequence homology (31% identity) over residues 2−269 (out of 278) with the protein YddE, PDB file 1P9V. The sequence for PhzF was imposed onto the YddE structure using Swiss-PdbViewer (*14*), and the worst side chain clashes were eliminated using the graphics program XtalView (*15*). Using this model and the program AMORE (*16*), we attempted molecular replacement. Since the space group was either $P3_1$-21 or $P3_221$, the molecular replacement program was run for both space groups. The best solution was obtained for space group $P3_221$. The refinement program REFMAC5 (*17*) was used to refine the model against the X-ray data; however, the refinement did not converge, and viewing the electron density map was inconclusive as to how to improve the fit.

Table 1: Data Collection and Refinement Statistics

space group	$P3_221$
cell dimensions (*a*, *b*, *c*) (Å)	56.22, 56.22, 155.06
resolution limit (Å)	1.8
no. of measured intensities	133,843
no. of unique reflections	27 247
mean redundancy	4.9
R_{merge} (overall/high-resolution shell)	0.047/0.175
completeness (overall/high-resolution shell)	99.7/96.9
average I/σ (overall/high-resolution shell)	19.4/4.7
refinement	
resolution limits (Å)	1.8
R-factor (95% of the data)	0.186
R_{free} (5% of the data)	0.222
no. of nonprotein molecules (not water)	2 sulfate ions
no. of water molecules	253
bond length rms deviation (Å)	0.019
angle distance rms deviation (Å)	1.84
average *B* (main chain/side chain) ($Å^2$)	20.4/24.1
average *B* for water ($Å^2$)	33.2

The program RESOLVE (*18*) was used with the partially refined model as the beginning model in a script for iterative automatic model building and composite-prime-and-switch-omit map calculation (http://resolve.lanl.gov/) to minimize phase bias of the molecular replacement solution. The initial build gave an *R*-factor of 0.497 and R_{free} of 0.569; the 43rd cycle gave an *R*-factor of 0.318 and R_{free} of 0.349 and built 256 residues, all with side chains. With the use of XtalView (*15*), the missing residues, which were mainly in turns, were easily built, and REFMAC5 was again used for refinement against the X-ray data. The usual cycling between refinement and model adjustment in the graphics resulted in a complete model with the statistics shown in Table 1.

RESULTS

Overall Structure. Crystals of PhzF diffracted well, and electron density is seen for the entire polypeptide chain but not for any of the intact his-tag. One residue, S213, is modeled in two conformations. The Ramachandran plot has 92.2% of the residues in the most favored region and 7.8% in the additional allowed region.

The structure of PhzF is composed of two domains, which have the same fold. The domains are connected by residues 119−122 and by a final β strand, which spans both domains. The CATH protein structure classification web site (http://www.biochem.ucl.ac.uk/bsm/cath) designates this mainly β-sheet fold as a roll. In PhzF, the core β-sheet of 16 β-strands runs continuously across the two domains wrapping around the two internal helices (α2 and α6), while the four remaining helices are located on the surface of the protein (Figure 1). There is a pronounced cleft where the two domains meet, and the N-terminal ends of the two internal helices are located at the back of this cleft. The dimensions of each monomer are approximately 50 Å × 35 Å × 35 Å, and each domain is approximately 25 Å × 35 Å × 35 Å. The rmsd between the Cα atoms of the two domains is 2.8 Å.

Active Site. At the junction of the two domains is a cleft approximately 14 Å deep, 8 Å in length, and just under 4 Å wide. A sulfate ion at the bottom of the cleft is within hydrogen bonding distance of the backbone nitrogen atoms of G73, H74, G212, and S213, ND1 of H74, and OG of S213 (Figure 2). Visual inspection of this deep cleft and the

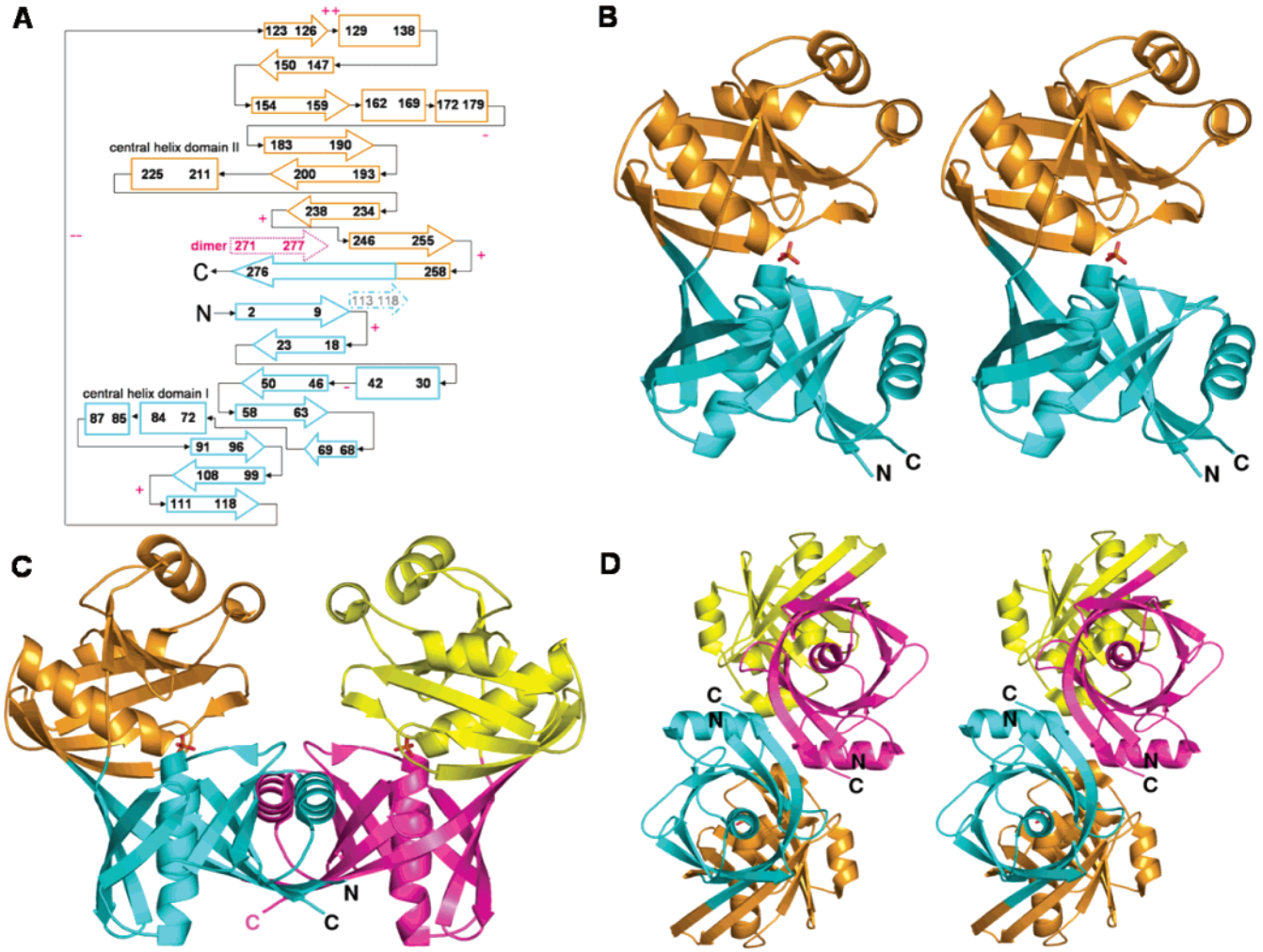

FIGURE 1: Schematic illustration of the secondary structural elements of PhzF and cartoon representations of the PhzF monomer and dimer. Panel A presents a secondary structure diagram of PhzF monomer. The structural elements belonging to domain I are outlined in cyan and those belonging to domain II are outlined in gold. β-strands are shown as arrows and α-helices are shown as rectangles. In domain I, a portion of the last β-strand interacts in an antiparallel fashion with a portion of the terminal β-strand of the molecule; this is shown as a dotted cyan arrow. A portion of the terminal strand from the dimer molecule is show in hot pink because it interacts in an antiparallel fashion with the first monomer. The red pluses and minuses indicate connecting regions where PhzF differs from the structure of DAP epimerase; the plus indicates that the PhzF structure has more residues in this connecting region, and the minus indicates that the PhzF structure has fewer residues. Panel B presents a stereoview of the monomer emphasizing the cleft between the domains. Again domain I is cyan, and domain II is gold. The sulfate ion found in the bottom of the cleft is shown as a stick model. Panel C presents a view of the dimer looking perpendicular to the 2-fold axis. In the second monomer, domain I is colored hot pink, and domain II is colored yellow. Panel D presents a stereoview of the dimer colored in the same fashion as the previous panel. This view emphasizes the continuation of the β-sheet across the dimer interface. It also provides a good view of the domain structure of a central helix wrapped in an eight-stranded mixed β-sheet.

fact that the DAP epimerase active site is in an analogous location, suggests that this is the active site. Modeling experiments with DHHA suggest two residues, E45 and D208, that could function as catalytic residues in an isomerization reaction, similar to C73 and C217 in DAP epimerase (see Discussion). In the crystalline state, access to the putative active site is limited suggesting that open and closed conformations exist, possibly modulated by movement of the domains relative to each other as has been suggested for the YddE protein (*19*).

Dimer Interface. The molecule forms a dimer with an interface that buries 2360 Å^2 of total surface area. In forming the dimer, the end (residues 271−277) of the final β-strand (β16) of each monomer interacts in an antiparallel fashion to make a continuous β-sheet going from one monomer to the other monomer. There are also significant contacts between helix 1 (residues 33−42) and residues on β1, β16, and several loop regions with R39 and D40 in particular making potentially important contacts with the opposing subunit. R39 interacts strongly with the backbone oxygen atoms of G243 and R244, ordering the potentially flexible loop element between β15 and β16, whereas the D40 carboxylate is strongly hydrogen-bonded (2.4 Å) to the D8 carboxylate on β1. The residues of the two α5 helices also interact and may tie together the portions of the monomers most distant from the primary interface region. (Figure 1C). The α5 helices are the only portions of domain II that exhibit interchain contacts. In the dimer, the proposed active site clefts open into a central cavity but are not spatially close together. Laser light scattering in solution yields a molecular mass of 66 070 ± 470 Da, roughly twice the monomer mass of 32 218 Da for histidine-tagged PhzF.

Structure Relatives. Automated superposition of the refined PhzF structure using the program DALI (*20*) revealed

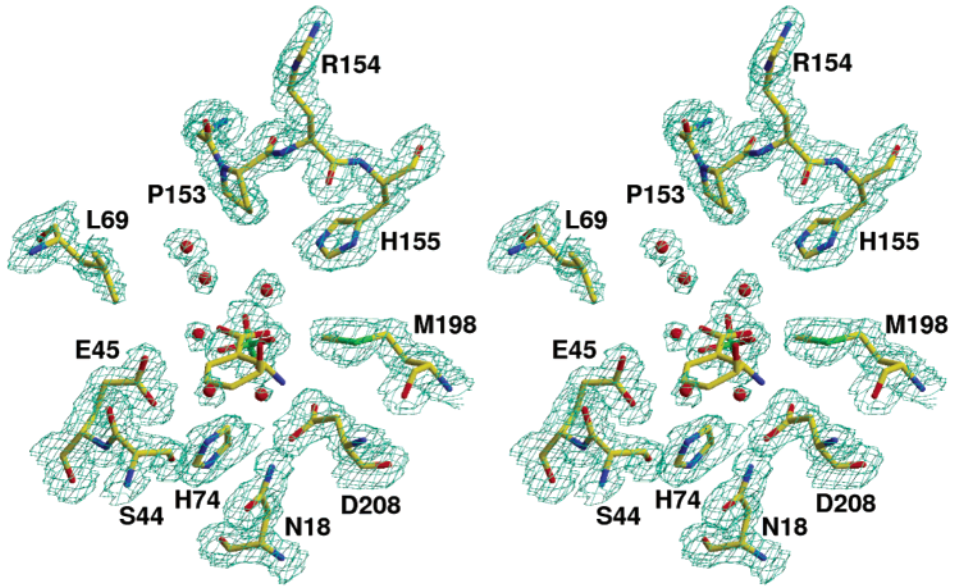

FIGURE 2: Representative electron density in the region of the proposed active site cleft of PhzF. The active site is shown occupied by a model of the substrate, DHHA. E45 and D208 could act as general acid−base catalysts in such a complex yielding the ketone as shown in Scheme 2. The σ-A weighted $2F_o - F_c$ electron density is shown contoured at 1σ.

Table 2: Results of DALI Search for Proteins Similar to PhzF

PDB entry	protein	DALI *Z* score	rmsd (Å)	no. of aligned residues	% sequence identity
1P9V	Ydde (orfb), *E. coli*	33.9	2.1	271	31
1S7J	phzF[a], *En. faecalis*	30.8	2.3	255	29
1BWZ	diaminopimelate epimerase	20.9	3.1	235	15
1I74	probable manganese-dependent inorganic pyrophosphatase	3.1	3.3	63	13
1O10	hypothetical protein af2198	2.6	2.7	60	8

[a] Possible misleading annotation, since *Enterococcus* is not known to produce phenazines.

significant similarity with only three structures, the YddE structure, which was used in the molecular replacement, diaminopimelate (DAP) epimerase (PDB code 1BWZ), and a protein annotated as PhzF from *Enterococcus feacalis* (PDB code 1S7J; Table 2). Since *Escherichia* and *Enterococci* species are not known to produce phenazines, these proteins likely have alternate functions and may be misannotated. Indeed sequence analysis with BLAST (*6*) suggests that the PhzF/DAP epimerase fold is widespread even though until quite recently the structure of only DAP epimerase was known. Structural alignment of PhzF and DAP epimerase is complicated by the presence of an active site disulfide bond in DAP epimerase, which distorts the architecture of the active site of that protein by pulling the two loop elements containing C73 and C217 close together. Because DAP epimerase functions via general acid−base catalysis involving the two cysteines, the structure of oxidized DAP epimerase may not provide an ideal structural comparison with PhzF, particularly in the active site region. In the reduced state, or in an enzyme−substrate complex, DAP epimerase may exhibit greater similarity to PhzF. Otherwise, the notable difference between PhzF and DAP epimerase includes 13 extra meandering residues in DAP epimerase in what corresponds to β9 of PhzF and a smaller stretch of 7−8 extra residues in DAP epimerase that corresponds to the regions following α1 and α5 of PhzF. Additionally, the loop regions in domain II of PhzF generally contain fewer residues than the corresponding loops in DAP epimerase, and PhzF lacks a six residue loop that follows β1 in both proteins.

In Vitro Activity of Phz Proteins. Biochemical experiments using lysates from cells that expressed the phenazine biosynthetic gene cluster from *P. fluorescens* 2-79 showed that PCA could be produced from ADIC. However, rapid metabolism of chorismate by host enzymes and possible complementation by host enzymes of selected genes that were deleted in various constructs complicated an unambiguous assignment of the functional characteristics of the individual Phz proteins (*9*). In an effort to gain further insight into the enzymology of phenazine biosynthesis, a series of enzymological reactions were carried out. In the first set of reactions, purified DHHA was incubated with a mixture of PhzA, -B, -G, and -F, and the products were analyzed. NMR (Table 3), MS ($m/z_{calcd} = 224.06$, $m/z_{obsd} = 225$, positive ion mode), and UV spectrometry (abs maxima 251 and 364 nm) confirmed that PCA was indeed formed in the presence of the four proteins. The conversion was rapid and quantitative as judged by UV spectroscopy and HPLC analysis.

Once the formation of PCA from the four proteins was confirmed, a second series of experiments was performed in which reactions lacking one or more of the proteins were analyzed in an attempt to establish the individual role of each protein. UV spectroscopy and HPLC revealed that PhzA, -B, and -G had no detectable activity toward DHHA either alone or in combinations with each other. By contrast, incubation of PhzF with purified DHHA resulted in the rapid depletion of substrate as monitored by UV spectroscopy (Figure 3A) or HPLC. Surprisingly, extended incubation of PhzF with DHHA led to a species with a UV spectrum consistent with PCA; however, the appearance of product did not correlate with DHHA consumption, suggesting a long-lived intermediate. The featureless UV spectrum of the species was consistent with a compound lacking the conju-

Table 3: NMR Assignments[a] for Phenazine-1-carboxylate

position	^{1}H[b]	^{13}C
1		125.0
2	9.01, dd, 1H	137.7
3	8.0, m, 3H	130.7
4	8.55, dd, 1H[c]	135.4
4a		144
5a		144
6	8.36, dd, 1H	130.4
7	8.0, m, 1H	132.1
8	8.0, m, 1H	133.5
9	8.30, dd, 1H[c]	128.4
9a		140
10a		139.8
carbonyl		166.5

[a] Chemical shift assignments for the unsubstituted ring are based on the expected incorporation of deuterium at C9. If C6 is the site of deuterium incorporation, shifts for C7 and C8 would be reversed. [b] Chemical shifts in ppm relative to TMS, multiplicity (dd = double doublet, m = multiplet), integral. [c] These resonances are absent and C2 becomes a simple doublet when PCA is produced in D_2O.

gated π electron system seen in DHHA and related chorismate derivatives. Evidence for the reactivity of the proposed intermediate was obtained by treating a solution of DHHA briefly with PhzF, quenching the reaction by addition of HCl, removing the PhzF by ultrafiltration, neutralization, and then adding PhzA, -B, and -G back to the solution alone and in various combinations. When PhzA, PhzB, or both were added back to the intermediate, a species with a UV spectrum characteristic of phenazine compounds but not identical to PCA was formed (Figure 3B). Furthermore, addition of PhzG, along with PhzA, PhzB, or both, enhanced the rate of product formation and led to a species with properties that were consistent with authentic PCA (Figure 3B, inset).

A third series of experiments was performed to assess the ability of PhzF alone to generate PCA. Analysis of the products of an overnight incubation of PhzF with DHHA by NMR, UV, and MS again confirmed the formation of PCA. HPLC analysis and NMR suggested that while PCA was the major product, other unidentified products were present as well.

Deuterium Incorporation. Reactions containing either PhzF alone or all four proteins were run in H_2O and in D_2O. The product molecular weights from the reactions run in H_2O were 225, as expected for PCA. When D_2O was used, the molecular weight of the product was 227, suggesting 2 mol of deuterium was incorporated in each mole of product. The deuterium atoms were shown to be in nonexchangeable positions by hydrating the product in a protiated solvent, drying, and reanalyzing by MS. Also, ^{1}H NMR spectra of PCA produced in D_2O lack the doublets at 9.01 and 8.30 ppm (Figures 4 and 5). Two-dimensional NMR experiments, in particular the HMBC experiment (Figure 4), which easily detects the strong $^3J_{CH}$ couplings in phenazines, demonstrate conclusively that C4 of PCA is the site of one deuteron when PCA is produced in D_2O since the proton signal at 8.55 ppm exhibits no cross-peak to the carbonyl carbon signal at 166.5 ppm, whereas the resonance at 9.01 ppm does show a cross-peak to the carbonyl carbon.[3] This strongly suggests that the proton with the 9.01 ppm resonance is three bonds removed from the carbonyl and is therefore H2. Deuteration at C4 is consistent with a C3 ketone in equilibrium with the corresponding enol and deuterium incorporation at C4 via

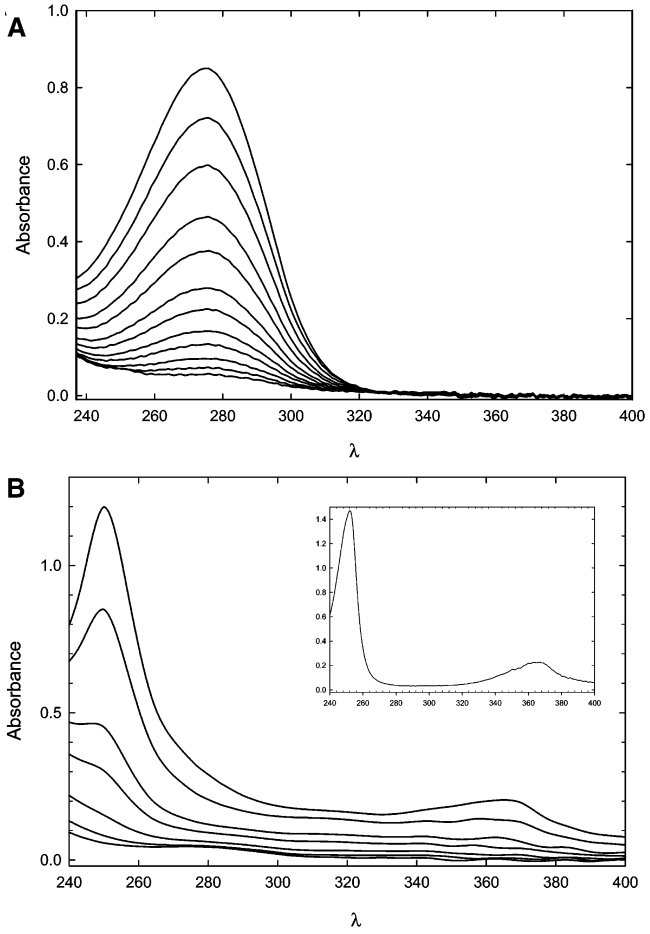

FIGURE 3: Panel A shows consumption of DHHA by PhzF. UV spectra of ~100 μM DHHA (top spectrum) are shown before and after addition of 500 nM PhzF to both the sample and reference cuvettes. Spectra were recorded at approximately 1 min intervals in 0.05 M KH_2PO_4 (pH 7.4). Panel B shows the action of PhzB on the compound produced by the action of PhzF on DHHA. UV spectra of the product of the PhzF reaction with DHHA (bottom spectrum) are shown. PhzF was removed from the solution by filtration before the spectrum was acquired. Subsequent spectra were recorded at ~5 min intervals after the addition of 200 nM PhzB protein to both sample and reference cuvettes. The inset shows the spectrum of 10 μM PCA produced by incubation of DHHA with PhzA, -B, -G, and -F (~100 nM each) for 5 min.

tautomerzation. Although, definitive NMR assignments for the unsubstituted ring of PCA are difficult to make, particularly with the small amounts of material in the current study, if deuterium is incorporated prior to dimerization (as described above), the location of the second deuteron is anticipated to be at C9. Deuteration at C6 cannot be ruled out however, and thus, the NMR assignments for the protons on C6/9 and C7/8 could be reversed.

DISCUSSION

Biochemical analysis of several purified Phz proteins show that DHHA is the substrate for PhzF and thus PhzF is the

[3] Several conflicting structures of PCA with different NMR assignments for various monosubstituted phenazines have been reported (*22*−*25*). These discrepancies may be attributable to impurities in natural isolates, instrumental limitations, or even misinterpretation of NMR data. The NMR assignments presented here are consistent with those expected for PCA in terms of chemical shift, multiplicity, and connectivity and are also corroborated by a comparison to the partially deuterated sample.

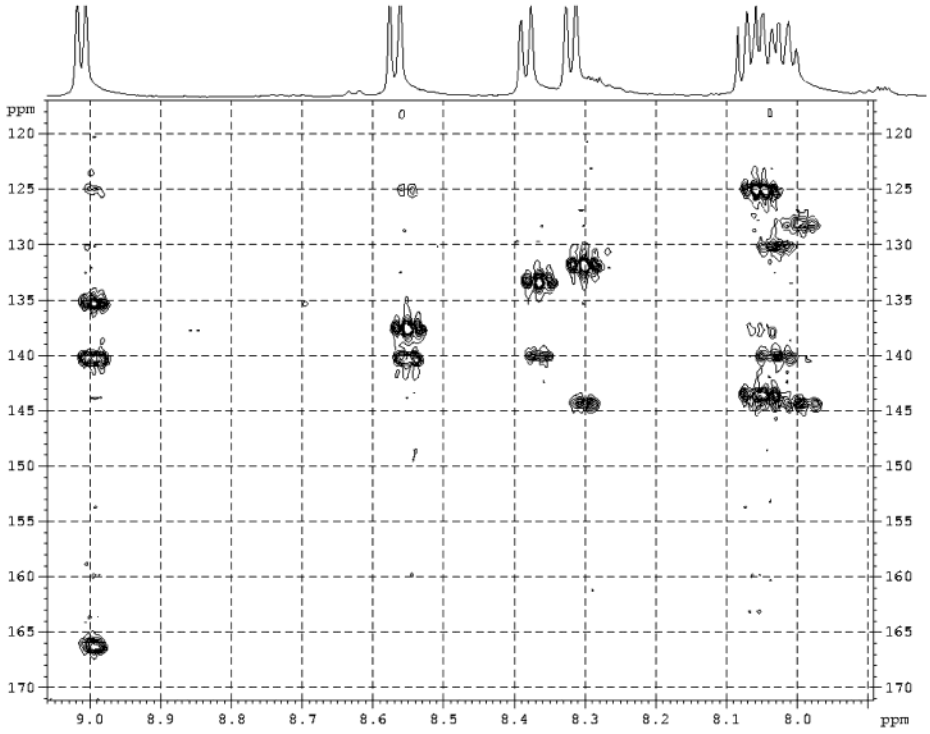

FIGURE 4: HMBC spectra. PCA extracted from a reaction initially containing DHHA, PhzA, -B, -C and, -G identifies this compound as PCA and confirms that the proton resonance at 8.55 ppm is H4 since only H2 exhibits three-bond correlation to the carbonyl carbon at 166.5 ppm. H4 (8.55 ppm) and H6 (8.30 ppm) are not present when the reaction is run in D_2O supporting the proposed involvement of a stable keto intermediate. The 1D proton spectrum of PCA is shown on the top axis. All proton and carbon chemical shift assignments are shown in Table 3.

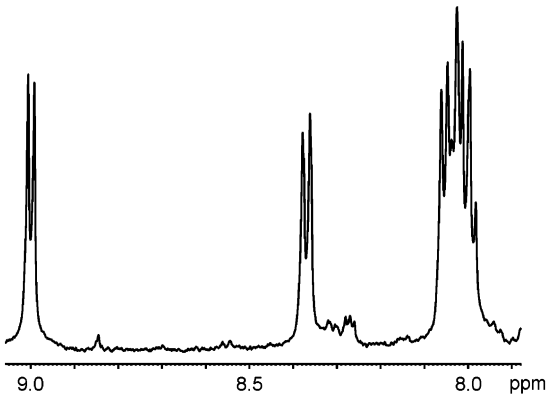

FIGURE 5: Deuterium incorporation suggests that PCA formation proceeds via a keto intermediate. The ^1H NMR spectrum of PCA extracted from a reaction initially containing DHHA (5 mM) and ~2 μM each PhzA, -B, -F, and -G in D_2O (20 mM KD_2PO_4, pD 7.5) is shown. The proton resonances at 8.55 and 8.36 ppm in Figure 4 are not evident in this spectrum suggesting that these positions become deuterated when the reaction is run in D_2O. Deuterium incorporation is proposed to be the result of keto−enol tautomerization prior to dimerization, as depicted in Scheme 2.

Scheme 2: A Possible Mechanism for PhzF-Catalyzed Allylic Rearrangement of DHHA

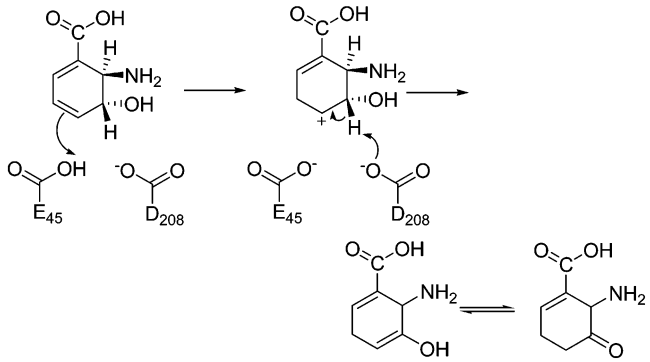

enzyme that catalyzes the first step in the dimerization of DHHA to PCA. McDonald and co-workers postulated that the most plausible mechanism for this reaction involves a ketone, and the evidence here supports that notion. However, our data suggests that direct oxidation of the C3 alcohol of DHHA is unlikely, given the inactivity of PhzG (a putative oxidase) toward DHHA and the consumption of DHHA by PhzF (Figure 3A). The intermediate formed by direct oxidation of C3 would, in the absence of unusual circumstances, quickly aromatize by tautomerization to 3-hydroxyanthranilic acid, a compound that has been ruled out as a phenazine precursor (*9*). A new proposal based on the data presented here is that PhzF catalyzes an allylic rearrangement, yielding a 3-oxo derivative of DHHA that is relatively stable (Scheme 2). Such a reaction would disrupt the conjugated diene system of the substrate, resulting in a less prominent UV signature as described above and as shown in Figure 3A. The formation of the 3-oxo product explains the facile incorporation of deuterium at C4 by tautomerization, and it would be reactive toward dimerization by two nucleophilic addition reactions, even in the absence of a catalyst. This explains the slow formation of PCA by PhzF alone, although the mechanism of decarboxylation of one ring is unclear. Finally, the fact that DAP epimerase is a known epimerase and that it is the only member of this fold family with a confirmed function supports the notion that PhzF catalyzes an isomerization as well.

Attempts to obtain a crystal structure of PhzF with bound substrate or product have been unsuccessful thus far, but

modeling of DHHA in the active site of PhzF yielded a possible bound conformation consistent with the proposed rearrangement mechanism (Figure 2). In this model, E45 would act as a general acid catalyst, donating a proton and facilitating formation of a carbocation at C4 of DHHA. D208 is then positioned to act as a general base that could abstract the C3 proton yielding, after tautomerization, the 3-oxo species of DHHA shown in Scheme 2. Interestingly, E45 and D208 appear to be invariant only among the sequences of PhzF homologues predicted to be involved in phenazine biosynthesis. On the basis of this mechanism, however, it is expected that deuterium would be incorporated into C3 and as well as C4 of oxidized DHHA and therefore found at C3, C4, C8, and C9 of PCA. By contrast, for reactions analyzed in the presence of PhzG, NMR data indicate that deuterium is found only at C4 and C9 of PCA. Therefore, barring an unlikely intramolecular allylic rearrangement, deuterium may indeed be incorporated at C4 and C5 of oxidized DHHA (and therefore C3, C4, C8, and C9 of PCA) and removed in a PhzG-catalyzed sterospecific oxidation step. This is feasible because the PhzG homolog, PdxH, has been shown to remove stereospecifically the proR hydrogen from C4′ of pyridoxine-5′-phosphate (*21*). Thus, when PCA is produced in D_2O, a deuteron may be incorporated at C5 of DHHA (C3/C8 of PCA) as depicted in Scheme 2 and removed in a PhzG-catalyzed stereospecific oxidation step.

One of the most intriguing, and poorly understood steps in phenazine biosynthesis is the dimerization of oxidized DHHA to generate a three ring structure. Is it possible that PhzF catalyzes two reactions, rearrangement and dimerization, perhaps even in a concerted process? This issue is currently difficult to resolve, especially since PCA and not phenazine-1,6-dicarboxylate was detected as the major product of the reaction containing only DHHA and PhzF. Interestingly, this observation suggests that PhzF may assist in the decarboxylation of oxidized DHHA or a tricyclic intermediate. On the other hand, a more attractive proposal is that PhzA and -B catalyze dimerization. PhzA and -B are encoded by the first two genes in this operon and are nearly identical in sequence yet have no other sequence homologues. Of course, this may simply reflect their role in catalyzing an unusual reaction such as phenazine ring formation. Indeed, the data in Figure 3B suggest but do not prove that PhzB, PhzA, or both facilitate the formation of the initial tricyclic species via dimerization of two rearranged DHHA molecules but do not shed light on why two copies of nearly identical proteins are required for efficient PCA production. Clearly additional structure−function analyses of the phenazine biosynthetic enzymes are needed to resolve the biochemical mechanisms of formation of these interesting and important compounds.

ACKNOWLEDGMENT

We thank Martin Safo and Verne Schirch at Virginia Commonwealth University for their help in assaying PhzG for pyridoxine oxidase activity and for helpful suggestions. We thank John Marino and John Orban for advice on NMR experiments.

REFERENCES

1. Mavrodi, D. V., Bonsall, R. F., Delaney, S. M., Soule, M. J., Phillips, G., and Thomashow, L. S. (2001) Functional analysis of genes for biosynthesis of pyocyanin and phenazine-1-carboxamide from *Pseudomonas aeruginosa* PAO1, *J. Bacteriol. 183*, 6454−6465.
2. Laursen, J. B., and Nielsen, J. (2004) Phenazine Natural Products: Biosynthesis, Synthetic Analogues, and Biological Activity, *Chem. Rev. 104*, 1663−1686.
3. Walsh, C. T., Liu, J., Rusnak, F., and Sakaitani, M. (1990) Molecular Studies on Enzymes in Chorismate Metabolism and the Enterobactin Biosynthetic Pathway, *Chem. Rev. 90*, 1105−1130.
4. Mavrodi, D. V., Ksenzenko, V. N., Bonsall, R. F., Cook, R. J., Boronin, A. M., and Thomashow, L. S. (1998) A seven-gene locus for synthesis of phenazine-1-carboxylic acid by *Pseudomonas fluorescens* 2-79, *J. Bacteriol. 180*, 2541−2548.
5. Wu, J., Howe, D. L., and Woodard, R. W. (2003) *Thermotoga maritima* 3-deoxy-D-arabino-heptulosonate 7-phosphate (DAHP) synthase: the ancestral eubacterial DAHP synthase? *J. Biol. Chem. 278*, 27525−27531.
6. Altschul, S. F., Madden, T. L., Schaffer, A. A., Zhang, J., Zhang, Z., Miller, W., and Lipman, D. J. (1997) Gapped BLAST and PSI−BLAST: a new generation of protein database search programs, *Nucleic Acids Res. 25*, 3389−3402.
7. Morollo, A. A., Finn, M. G., and Bauerle, R. (1993) Isolation and Structure Determination of 2-Amino-2-deoxyisochorismate: An intermediate in the Biosynthesis of Anthranilate, *J. Am. Chem. Soc. 115*, 816−817.
8. Parsons, J. F., Calabrese, K., Eisenstein, E., and Ladner, J. E. (2003) Structure and mechanism of *Pseudomonas aeruginosa* PhzD, an isochorismatase from the phenazine biosynthetic pathway, *Biochemistry 42*, 5684−5693.
9. McDonald, M., Mavrodi, D. V., Thomashow, L. S., and Floss, H. G. (2001) Phenazine biosynthesis in *Pseudomonas fluorescens*: branchpoint from the primary shikimate biosynthetic pathway and role of phenazine-1,6-dicarboxylic acid, *J. Am. Chem. Soc. 123*, 9459−9460.
10. Cirilli, M., Zheng, R., Scapin, G., and Blanchard, J. S. (1998) Structural symmetry: the three-dimensional structure of Haemophilus influenzae diaminopimelate epimerase, *Biochemistry 37*, 16452−16458.
11. Bax, A., and Summers, M. F. (1986) 1H and 13C assignments from sensitivity enhanced detection of heteronuclear multiple-bond connectivity by two-dimensional multiple quantum NMR, *J. Am. Chem. Soc. 108*, 2093−2094.
12. Pflugrath, J. W. (1999) The finer things in X-ray diffraction data collection, *Acta Crystallogr. D55*, 1718−1725.
13. Berman, H. M., Westbrook, J., Feng, Z., Gilliland, G. L., Bhat, T. N., Wieissig, H., Shindyalov, I. N., and Bourne, P. E. (2000) The Protein Data Bank, *Nucleic Acids Res. 28*, 235−242.
14. Guex, N., and Peitsch, M. C. (1997) SWISS-MODEL and the Swiss-PdbViewer: An environment for comparative protein modeling, *Electrophoresis 18*, 2714−2723.
15. McRee, D. E. (1999) *Practical Protein Crystallography*, 2nd ed., Academic Press, San Diego.
16. Navaza, J. (1994) AMoRe: an automated package for molecular replacement, *Acta Crystallogr. A50*, 157−163.
17. Murshudov, D. N., Vagin, A. A., and Dodson, E. J. (1997) Refinement of Macromolecular Structures by the Maximum-Likelihood Method, *Acta Crystallogr. D53*, 140−255.
18. Terwilliger, T. C. (2003) Automated main-chain model building by template matching and iterative fragment extension, *Acta Crystallogr. D59*, 38−44.
19. Grassick, A., Sulzenbacher, G., Roig-Zamboni, V., Campanicci, V., Cambillau, C., and Bourne, Y. (2004) Crystal Structure of E. coli YddE Protein Reveals Striking Homolgy with Diaminopimelate Epimerase, *Proteins 55*, 764−767.
20. Holm, L., and Sander, C. (1995.) Dali: a network tool for protein structure comparison, *Trends Biochem. Sci. 20*, 478−480.
21. di Salvo, M. L., Ko, T. P., Musayev, F. N., Raboni, S., Schirch, V., and Safo, M. K. (2002) Active site structure and stereospecificity of *Escherichia coli* pyridoxine-5′-phosphate oxidase, *J. Mol. Biol. 315*, 385−397.
22. Breitmaier, E., and Hollstein, U. (1976) Carbon-13 Nuclear Magnetic Resonance Chemical Shifts of Substituted Phenazines, *J. Org. Chem. 41*, 2104−2108.
23. Brisbane, P. G., Janik, L. J., Tate, M. E., and Warren, W. F. O. (1987) Revised Structure for the Phenazine Antibiotic for *Pseudomonas fluorescens* 2-79 (NRRL B-15132), *Antimicrob. Agents Chemother. 31*, 1967−1971.

24. Romer, A. (1982) 1H NMR Spectra of Substituted Phenazines, *Org. Magn. Reson. 19*, 66−69.
25. Gurusiddaiah, S., Weller, D. M., Sarkar, A., and Cook, R. J. (1986) Characterization of an Antibiotic Produced by a Strain of *Pseudomonas fluorescens* Inhibitory to *Gaeumannomyces graminis* var. tritici and *Pythium* spp., *Antimicrob. Agents Chemother. 29*, 488−495.

BI049059Z